Dynamics of fluid and heat flow in a CO_2-based injection-production geothermal system

FENG Guan-hong, XU Tian-fu*, ZHU Hui-xing

Key Laboratory of Groundwater Resources and Environment, Ministry of Education, Jilin University, Changchun 130021, China.

Abstract: CO_2 is now considered as a novel heat transmission fluid to extract geothermal energy. It can be used for both energy exploitation and CO_2 geological sequestration. Here, a 3-D, "two-spot" pattern well model is developed to analyze the mechanism of CO_2-water displacement and heat extraction. To obtain a deeper understanding of CO_2-geothermal system under some more realistic conditions, heterogeneity of reservoir's hydrological properties is taken into account. Due to the fortissimo mobility of CO_2, as long as the existence of highly permeable zone between the two wells, it is more likely to flow through the highly permeable zone to reach the production well, even though the flow path is longer. The preferential flow shortens circulation time and reduces heat-exchange area, probably leading to early thermal breakthrough, which makes the production fluid temperature decrease rapidly. The analyses of flow dynamics of CO_2-water fluid and heat may be useful for future design of a CO_2-based geothermal development system.

Keywords: Binary system; CO_2-water displacement; Heterogeneity; Preferential flow

Introduction

The Enhanced Geothermal System (EGS) is defined as an engineered reservoir that has been created to extract economical amounts of heat from geothermal resources of low permeability and/or porosity (Tester J W *et al*. 2006). As part of an effort to reduce atmospheric emissions of carbon dioxide (CO_2), a novel concept of operating the EGS using CO_2 instead of water as the working fluid (CO_2-EGS) and achieving simultaneous geologic sequestration of CO_2 has been proposed and evaluated (Brown D W, 2000; Pruess K, 2006).

In recent years, a similar concept, the so-called CO_2-Plume Geothermal (CPG) system, has been proposed (Randolph J B and Saar M O, 2011). The CPG system utilizes existing, naturally porous, and highly-permeable geologic formations (reservoirs) for geothermal energy recovery. The major benefit of the CPG system over the EGS is that the CPG system does not require hydro-fracturing, which helps increase fracture permeability but may induce seismicity. The EGS has encountered considerably unfavorable conditions and socio-political issues (resistances). Consequently, the CPG that can use the CO_2 sequestration site to recover geothermal energy may be practical. In this paper, CO_2-based geothermal system can be referred for both the CPG and the CO_2-EGS.

Pruess K (2006, 2008) performed fundamental numerical studies to evaluate the heat extraction performance of two fluids. He reached the conclusion that under certain thermal conditions, the heat extraction rate of CO_2 can be 50% higher than water. CO_2 fluid flow in wellbore was considered under some restrictions, or the flow in wellbore was treated as isenthalpic flow. The heat exchange between wellbore and surrounding geological formation was not considered, and Joule- Thomson effect in wellbore was noticed. It was concluded that the favorable properties for CO_2 are having (1) large expansibility, which would generate large density differences between injection and production wells, and provide buoyancy force and then reduce power

*Corresponding author. E-mail: Tianfu_xu@jlu.edu.cn

consumption, (2) lower viscosity, which would lead to a larger mass flow rate, and (3) lower reactivity, or, CO_2 is not likely to react with rock compared with water.

Atren A D *et al.* (2010) analyzed power generation from a doublet CO_2 geothermosiphon system without considering frictional effects, indicating that CO_2-EGS could generate similar amounts of power as a water-EGS, but with simpler surface equipment. Atren A D *et al.* (2010) took frictional loss into account, and indicated that the CO_2-EGS would be less effective for energy extraction than a water-EGS for conditions used in past EGS trials. They also discussed the effects of diameter of well and permeability of reservoir, and concluded that CO_2 is superior to water in lower permeability reservoir and larger wellbore. Previous studies discussed were performed under many restrictions especially for the flow in wellbore. The properties of CO_2 make the processes in the wellbore totally different from those in the reservoir. The previous wellbore-decoupled model could not capture important features of the entire processes. Pan L and Oldenburg C M (2014) developed a fully coupled wellbore-reservoir simulator called T2 well, which is based on TOUGH2 (Pruess K *et al.* 1999). The program considers the wellbore and reservoir as an integrated system. The program was used to study CO_2 and brine leakage along wellbore (Pan L and Oldenburg C M, 2011a). This coupled model is a significant advance for studies of CO_2 multiphase flow and thermodynamics in both wellbore and reservoir, and is a very useful tool for design and optimization of a CO_2-based geothermal system (Pan L *et al.* 2015). XU T *et al.* (2015) compared advantages of two heat transmission fluid using a "five-spot" well pattern, and drew the conclusion that CO_2 is more suitable for low permeability, and low temperature geothermal reservoir.

In this work, a more realistic well-reservoir coupled "two-spot" well pattern model is built. At first, a homogeneity case is used to analyze the basic mechanism and pressure profile of the system and discuss the suitable production pressure. A more complex model is then built to evaluate the influence of the heterogeneity of geological media on the dynamics of fluid and heat flow.

1 Problem setup

1.1 Model setup

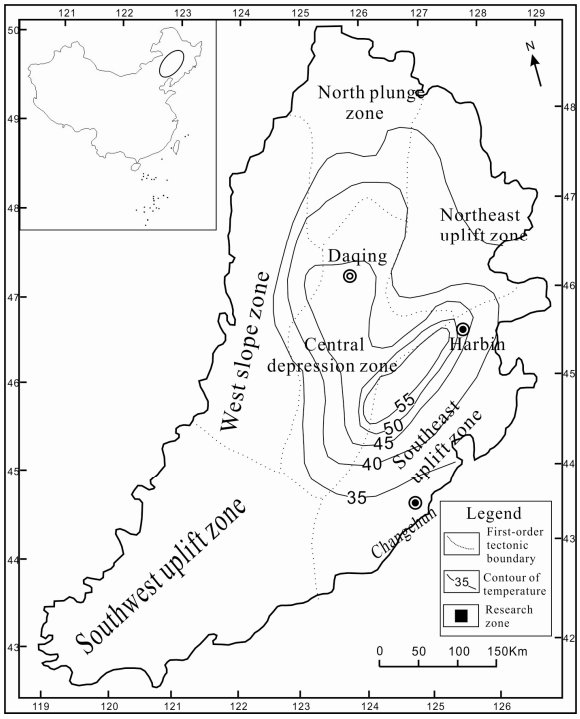

Fig. 1 Location of Songliao Basin, Northeastern China

A great deal of detailed information is required to assess the feasibility of injected CO_2 as a heat transmission fluid at any specific site, and to develop engineering designs for CO_2-based geothermal systems. Before moving into site-specific investigations, general features and issues should be explored. This can be done by investigating deep brine systems that abstract site-specific features and thereby attempt to represent characteristics that are common to many such systems. Here, geological characteristics and physic-thermo conditions are mainly extracted from the central depression of Songliao Basin, Northeastern China. The basin features the highest geothermal gradient and heat flow among sedimentary basins in China, and can meet the temperature requirement for geothermal development. We treat reservoir as a naturally porous media.

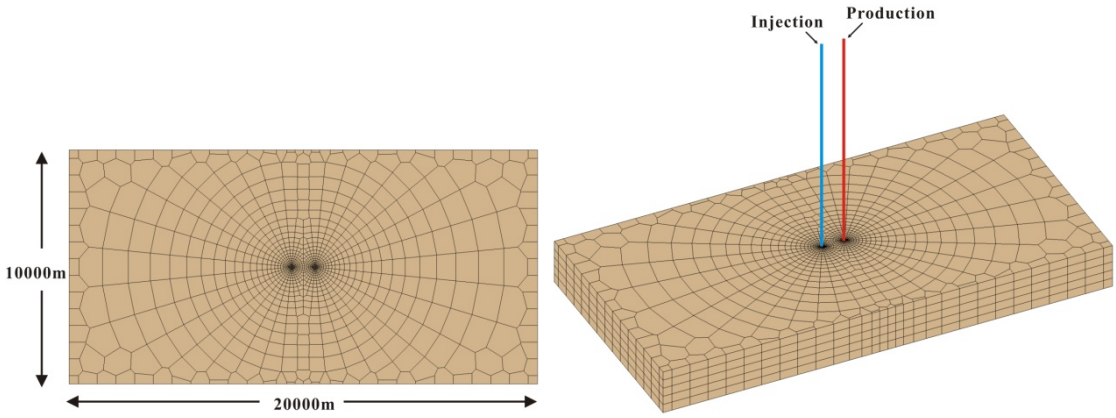

Fig. 2 Overview of the two-spot well pattern with computational grid (left) and 3-D sketch of the modeling grid (right)

In this study, a 3-D, "two-spot" pattern model is built, as shown in Fig. 2. The distance between two wellbores is 1 000 m, perforating both wellbores open to the reservoir layer. The heat exchange between wellbore and surrounding geological formation is calculated using a semi-analytical solution (Ramey Jr H J, 1962). The geological and thermo-physical conditions are extracted from the Songliao Basin site. The geothermal reservoir that authors of this paper considered is sandstone formation with a thickness of 100 m (Table 1), and the details of the model are listed in Table 1.

Table 1 Geometric and hydrogeological specifications for the simulation

Formation	
Thickness	100 m
Porosity	0.1
Permeability	3.2×10^{-14} m^2
Rock grain density	2650 kg/m^3
Rock specific heat	920 J/kg/°C
Rock thermal conductivity	2.51 W/m/°C
Pattern area	2×10^8 km^2
Injector-producer distance	1 000.0 m
Reservoir temperature	150 °C
Average reservoir pressure	36.7 MPa
Wellbores	
Diameter	0.2 m
Roughness	0.046 mm
Heat conductivity	2.51 W/m/°C
The inclination of wells	Vertical

1.2 Model Scenarios

Normally, the reservoir is initially saturated with resident water. The process of CO_2 displacing water will take quite a long time to dry the formation water out and to create a CO_2 dominating reservoir. To analyze the fluid and thermal dynamics of supercritical CO_2 displacing water, we started with a CO_2-water displacement model (Case 1). To displace the water out as soon as possible, a high pressure of 16.0 MPa is assigned for injection and an atmospheric pressure for production at the early stage. When CO_2 flows through, the density of fluid in production well may decrease drastically. To get a higher production fluid temperature and keep a stable operation

of the binary system, a much higher production pressure needs to be imposed after the production fluid is almost occupied by CO_2 (about after 8 years in this model). To analyze the mechanism and obtain a more optimal production condition, different cases of production pressure (10, 12, 14 MPa) are set and discussed (Table 2).

Table 2 Parameters for CO_2-water displacement model

Production/Injection	
Injection temperature	20 °C
Injection pressure	16.0 MPa
Production pressure	0.1 MPa (first 8 years) 10, 12, 14 MPa (8-30years)
Parameter for relative permeability (van Genuchten's model for liquid and Corey's model for gas)	
Residual liquid saturation	0.15
Residual gas saturation	0.01
Saturated liquid saturation	1.00
mVG	0.65
Parameter for capillary pressure (van Genuchten's model)	
Residual liquid saturation	0.03
Saturated liquid saturation	1.00
mVG	0.4118
Alpha	6.08×10^{-5} Pa^{-1}
Maximum capillary pressure	6.4×10^{7} Pa

1.3 Simulation approach

The CO_2-water multi-phase flow processes have been modeled with the fully coupled wellbore-reservoir simulator-T2Well. It is developed by introducing wellbore flow equations into the reservoir simulator TOUGH. In the T2Well, the matrix assembling for wellbores and reservoir are based on different governing equations. The flow process in the reservoir is based on regular Darcy's law, while the flow in wellbores is governed by 1-D momentum conservation equation (Pan L *et al*. 2011b). The main variable is the mixture velocity, and Drift-flux model is introduced to calculate the velocity for each phase.

2 Results and discussion

2.1 Homogeneous cases

It can be seen that there exists two periods (Fig. 3a). In the first stage, most production fluid is water. After 8 years' operation, CO_2 is dominant in the production fluid. To keep a stable operation, and maintain CO_2 in supercritical state a much higher pressure is imposed to production wellhead. In the first period, it takes about one year for CO_2 to flow from injection well to production well (Fig. 3b). Once breakthrough occurs, the flow rate ascends rapidly because of the strong mobility of CO_2. At the same time, there is a decline of production temperature due to the Joule-Thompson effect. In the second stage, the gas saturation at the production wellhead is slightly lower than that in stage 1. CO_2 is accompanied by water during the whole production process, when it is extracted through the production well.

Two main indexes to assess a CO_2-geothermal system are heat extraction rate and production temperature. The evolutions of the parameters are shown in Fig. 4. According to Pruess K (2008), heat extraction rate is calculated as Eq.(1). The evolution of production fluid temperature and heat extraction rate is shown in Fig. 4. The production fluid temperature is proportional to the production pressure because of the Joule-Thompson effects. However, the heat extraction rate is opposite, and the reason is that higher production pressure corresponds to lower flow rates.

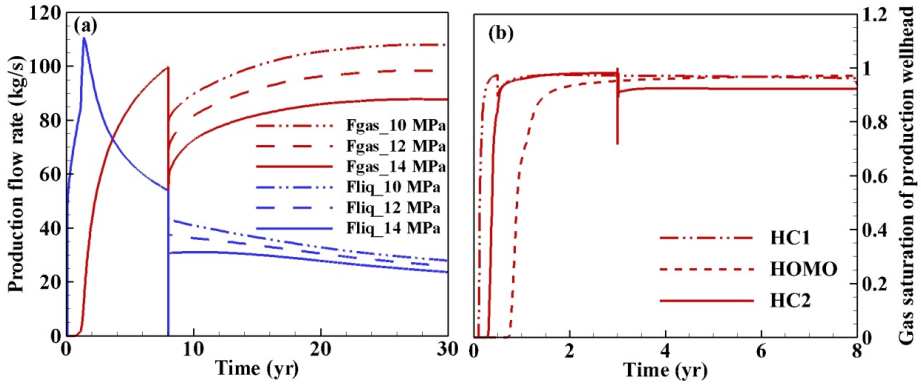

Fig. 3 Evolution of production flow rate (a) and gas saturation of production fluid (b)

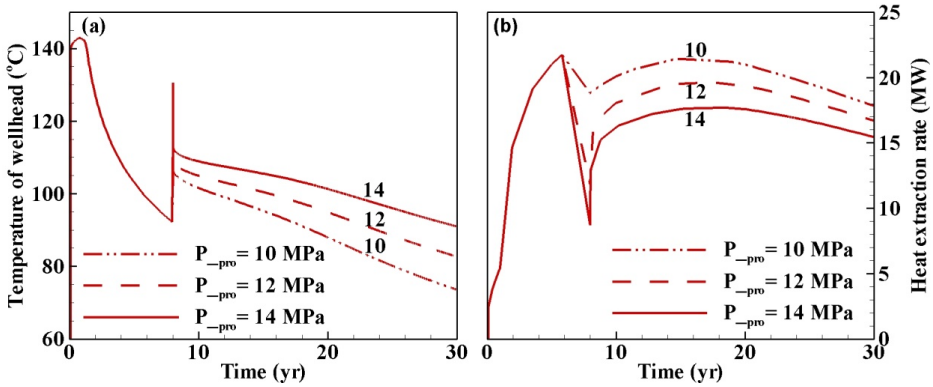

Fig. 4 Evolution of production fluid temperature and heat extraction rate

$$G = F_{pro}(h_{pro} - h_{inj}) \tag{1}$$

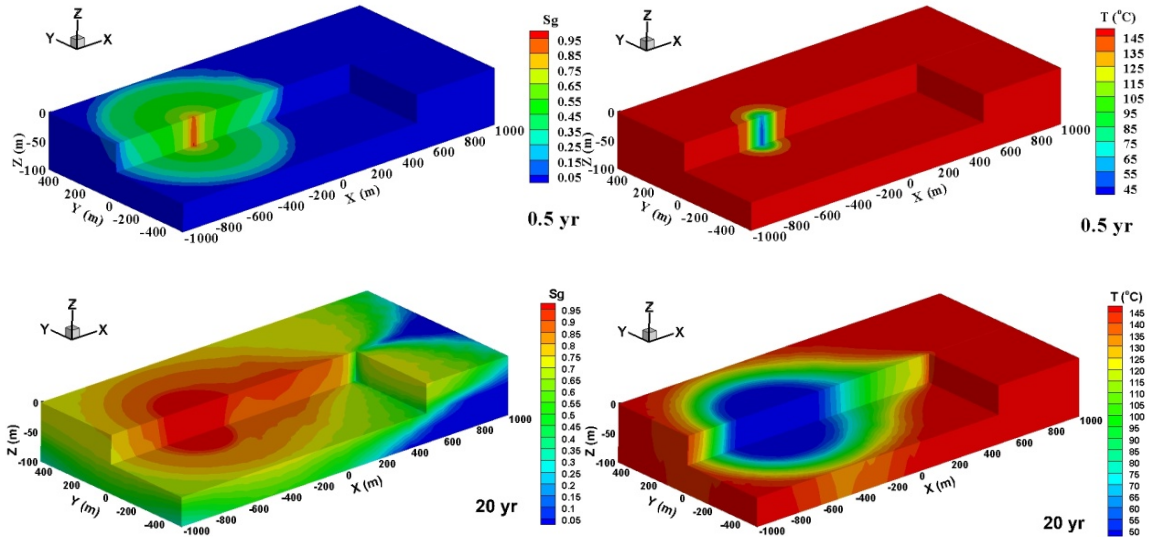

Fig. 5 Gas and temperature distribution after 0.5 and 20 years

The gas saturation and temperature distribution are shown in Fig. 5. To analyze the flow process in reservoir, the flow field is shown in Fig. 6. After 0.5 year's operation, the gas does not reach the production well, and production fluid is totally water. After 10 years' operation, most CO_2 flow along the direction from injection well to production well. The water of production fluid all comes from the opposite direction of injection well, and that's why the production fluid contains water during the whole operation process.

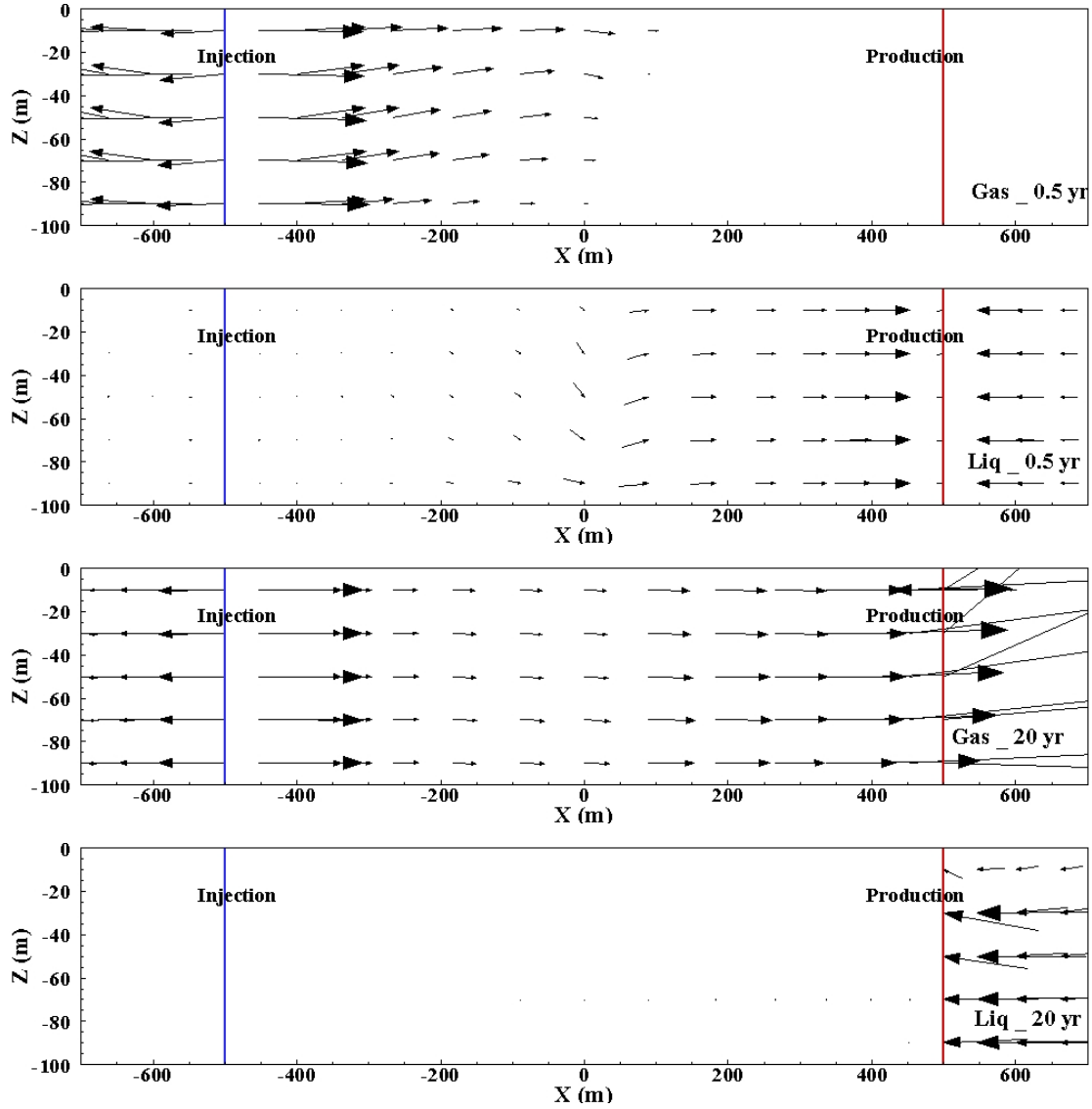

Fig. 6 The flow field for CO_2 and water after 0.5 year and 20 years

To obtain a deeper understanding of different cases, the pressure and specific enthalpy evolutions are analyzed. In T2Well simulator, the governing equations of multiphase flow in wellbores is described as Eq. (2),

$$\frac{\partial}{\partial t}(r_m u_m)+\frac{1}{A}\frac{\partial}{\partial z}[A(r_m u_m^2+g)]=-\frac{\partial P}{\partial z}-\frac{\Gamma f\, r_m |u_m| u_m}{2A}-r_m g\cos q \tag{2}$$

where, $g=\frac{S_G}{1-S_G}\frac{r_G r_L}{r_m^{*2}}[(C_0-1)u_m+u_d]^2$

where, u_m and r_m is the velocity and density of the mixture fluid, A is the cross sectional area of the wellbore, and Γ is the perimeter of the cross-section.

If we just focus on the pressure and enthalpy profile along the flow path at some specific time, the part in terms of time can be neglected. Eq. (2) can be simplified as Eq. (3). From Eq. (3), it can be seen that the pressure drop along wellbore includes three parts: ① The gravitational term; ② the frictional term; ③ the compressibility term. The pressure change due to three parts is shown in Table 3.

$$\frac{dP}{dz}=-r u\frac{du}{dz}-\frac{\Gamma f\, r |u| u}{2A}-r g\cos q \tag{3}$$

From Table 3, it can be seen that the pressure change due to compressibility is too small compared to other terms, and it is neglected in later discussions.

Table 3 Component pressure changes for two fluids

Pressure change (MPa) (Production/Injection)	Gravity	Friction	Compressibility
10 MPa	-17.65/35.16	-6.60/-2.83	-0.066/-0.018
12 MPa	-18.74/35.19	-5.14/-2.38	-0.048/-0.016
14 MPa	-19.81/35.22	-3.87/-1.92	-0.034/-0.013

The pressure change due to gravity in injection well is basically the same for all cases (Fig. 7). But that for production well is proportional to the production pressure, because higher production pressure corresponds to higher density of CO_2. Subsequently, higher production pressure leads to a lower velocity and frictional loss. The compressibility term is generated dominantly by the compressibility of CO_2, because its density is very sensitive to pressure and temperature.

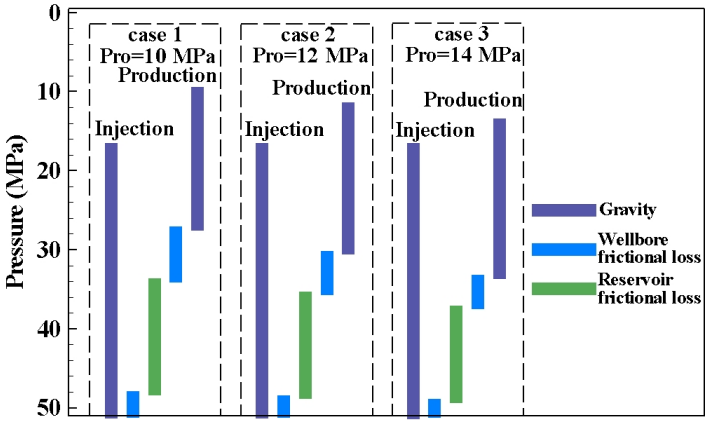

Fig. 7 Pressure changes along the wellbores and in the reservoir at 20 years for different production pressure cases

2.2 Heterogeneity effects

From a realistic view, natural aquifer is intrinsically heterogeneous. The fluids are more likely to flow through the highly permeable zones, especially for CO_2, because of its strong mobility. It may lead to an early breakthrough. Among the properties of reservoir, permeability and porosity have the largest influence on flow field and heat extraction. Therefore, we just take them as the main variables to study heterogeneity effects. Here, we take the 12 MPa production pressure case as the reference.

Based on the results of calculations with homogeneous distribution of hydrological and thermal parameters, a set of additional models were then run by assuming the permeability to be: (i) Lognormally distributed in a sub domain (Baecher G B and Christian J T, 2005; Haldar S and Babu G L S, 2008) (heterogeneous volume, hereinafter HV) , the coordinate is (-1 000, 1 000) along X direction, (-500, 500) along Y direction and (-100, 0) along Z direction; (ii) homogeneously distributed (Table 1) over the rest of the domain. Standard geostatistical techniques were then applied to this sub-domain, a mean permeability value of 5.0×10^{-14} m^2, and a variance of 1.35 (TIAN H *et al.* 2014) and the maximum and minimum of permeability are set 5.0×10^{-11} m^2 and 5.0×10^{-17} m^2, respectively. Permeability values were finally assigned by calculating a spherical semivarioram (Fig. 8) without nugget effect (C_0=0), with a sill of 1.35 (C=1.35). The correlation length strongly depends on the variogram type and the model scale (Srivastava A *et al.* 2010; TIAN H *et al.* 2014). Here, a correlation length of 375 m (a=375) is chosen, according to the following relationships:

$$\gamma(h) = \frac{1}{2} \times Var[Z(x) - Z(x+h)] = \frac{1}{2} \times E \times [Z(x) - Z(x+h)]^2 \quad (4)$$

$$\gamma(h) = \begin{cases} 0, & h = 0 \\ C_0 + C \times \left(\frac{3h}{2a} - \frac{h^3}{2a^3}\right), & 0 < h \le a \\ C_0 + C, & h \ge a \end{cases} \quad (5)$$

The semivariogram allows for a quantitative description of the spatial dependence of a randomly heterogeneous field (Curran P J, 1988; Zimmerman D L and Zimmerman M B, 1991). It is defined as the variance of the difference between any two spots in the field, as given by Eq (2). In this framework, x is a random spot in the field, h is the distance from x to any other spot, Z is the spatial variable (permeability in our case), $\gamma(h)$ is the correlation of any two spots, and higher $\gamma(h)$ values indicate weaker correlation degrees. A comparison between the permeability values is obtained by assuming a lognormal distribution of values, and those generated in our model by applying a geostatistical approach is given in Fig. 8. The initialization of the model was finalized by passing the permeability values calculated over the ECG to the HV sub-domain of the field-scale model, which has a different spatial discretization ($\Delta X = \Delta Y = \Delta Z = 25\text{m}$). This was done by adjusting (by kriging) the values computed over the ECG to the grid of the field-scale model (HV sub-domain).

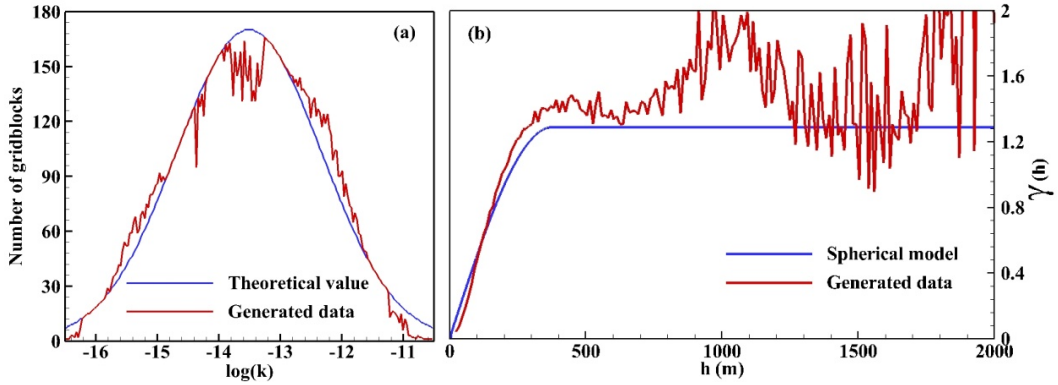

Fig. 8 (a) Lognormal distribution of permeability (variance:1.35; mean:5.0×10^{-14} m^2. (b) Experimental semivariogram (spherical model) inferred from 100 generated permeability values

The $\phi - k$ relation in geologic media depends on the intrinsically complex structure of the porous space, and particularly on the dimensions of connected pores/fractures (*e.g.*, Archie G E, 1959, 1952; Bear J, 1972). Although experimental observations and field logs have demonstrated that no single model can reliably describe this intrinsic complexity, different types of models have been proposed to link permeability and porosity values (*e.g.*, Carman P C, 1956; Katz A J and Thompson A H, 1986; Nelson P H, 1994; Timur A, 1968). Based on the qualitative observation that permeability values generally correlate with porosity values, here, for the sake of simplicity, authors of this paper assumed, according to the literature (Nelson P H, 1994), that these variables obey the following equation:

$$\log(k) = a \times \phi + b \quad (6)$$

where, k is the permeability (m^2) and ϕ is the porosity, a and b are two empirical coefficients set to 37.5 and -17.245 in the case of carbonate reservoirs (Davis S N, 1969; Ehrenberg S N and Nadeau P H, 2005). The minimum, average and maximum porosity values calculated with this equation for the Songliao Basin are 0.02, 0.1 and 0.18, respectively.

Infinite types of heterogeneous permeability fields can be generated by means of random number generators. In the following, only two selected cases are discussed as representative of the following limiting conditions: (i) High-permeability zone between the two wells (Fig. 9a, heterogeneous case 1, hereinafter HC1); (ii) low-permeability zone between the two wells (Fig. 9b; heterogeneous case 2, HC2). Although these are only a few possible realizations of the

subsurface structure, they are intrinsically not representative of any part of the reservoir, and they were used to explore the sensitivity of the numerical model and to quantify the effects of heterogeneities on the profitability of a CO_2-geothermal project with the extremities in porosity and permeability so far defined.

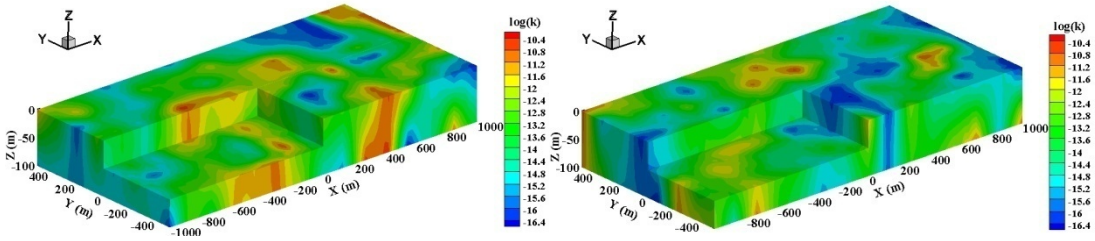

Fig. 9 Two hypothetical heterogeneous permeability distributions

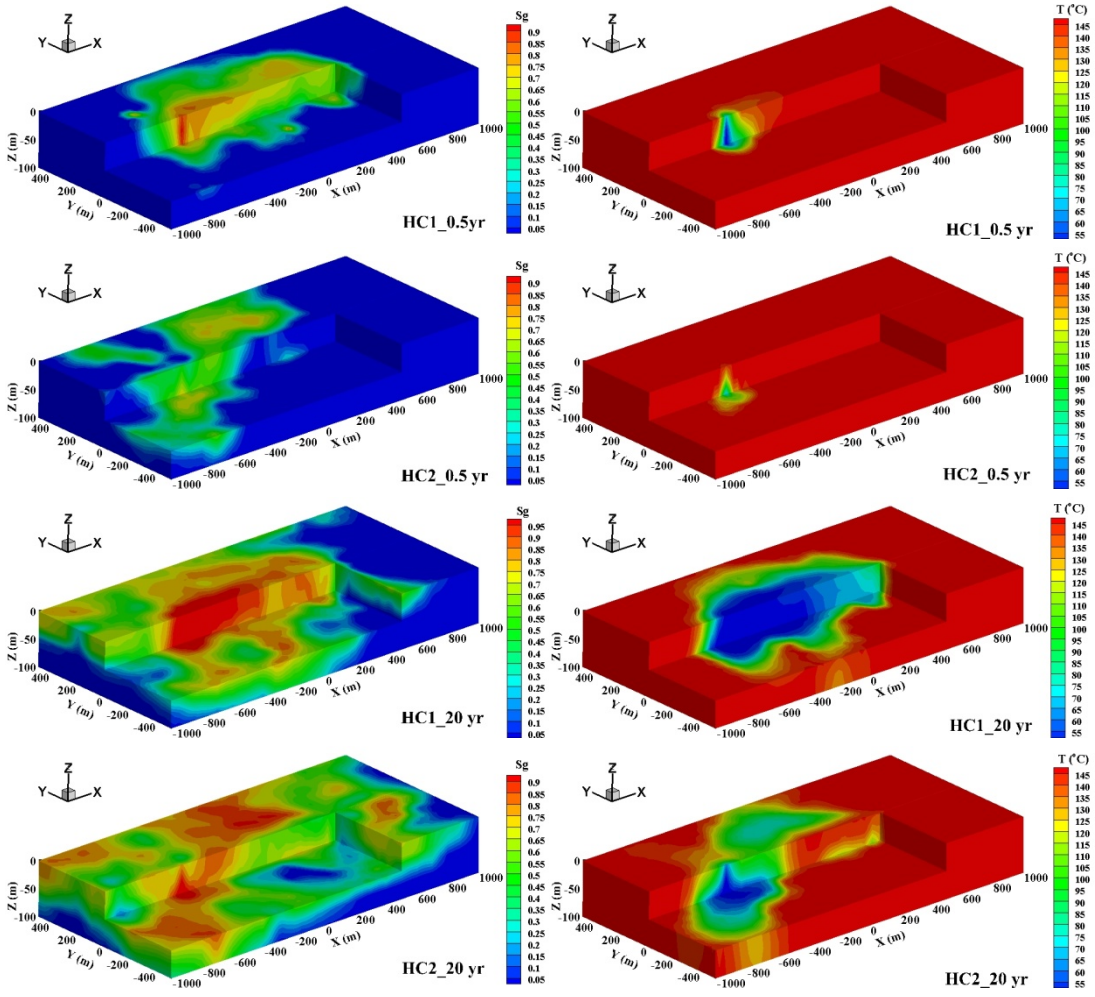

Fig. 10 Gas saturation and temperature distribution at 0.5 year and 20 years for heterogeneity cases

It can be seen from Fig. 10, heterogeneity can easily lead to an early breakthrough, and it only takes 0.1 year for CO_2 to reach the production well in HC1. Even for HC2, it is only 0.3 year, much shorter than that in homogeneity case (1.0 year). This is caused by the strong mobility of CO_2, in HC2, as long as there exists a highly permeable zone, it can bypass the low permeability zone to reach the production well (Fig. 10, HC2_0.5 yr). Consequently, the time for increasing the production pressure should also be earlier: 1 year for HC1 and 3 year for HC2.

The CO_2 flow rate is shown in Fig. 11. In homogeneity case, for injection well, we can see the CO_2 flow rate does not vary with depth, because of the buoyancy, most production CO_2 gathering in the top of reservoir. For heterogeneity case 1, due to the high permeability, the flow rate is higher than that of homo case. For heterogeneity case 2, there is nearly no flow rate in upper part of reservoir because of the low permeability of the top zone, where the CO_2 flow passes through the bottom of reservoir to reach production well.

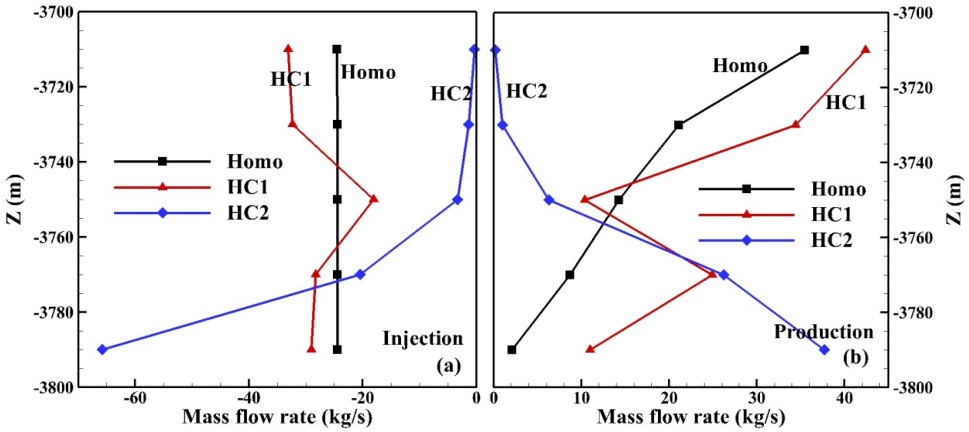

Fig. 11 The CO_2 mass flow rate of per 50 m thickness in reservoir for different cases

The CO_2 production flow rate is basically proportional to the permeability between the two wells (Fig. 12a). The flow rate of water in homogeneity case is much higher than that in heterogeneity cases while the flow rate of water is not. This is because the multi-phase fluids move as a whole in homogeneity, unlike the preferential flow in heterogeneity cases.

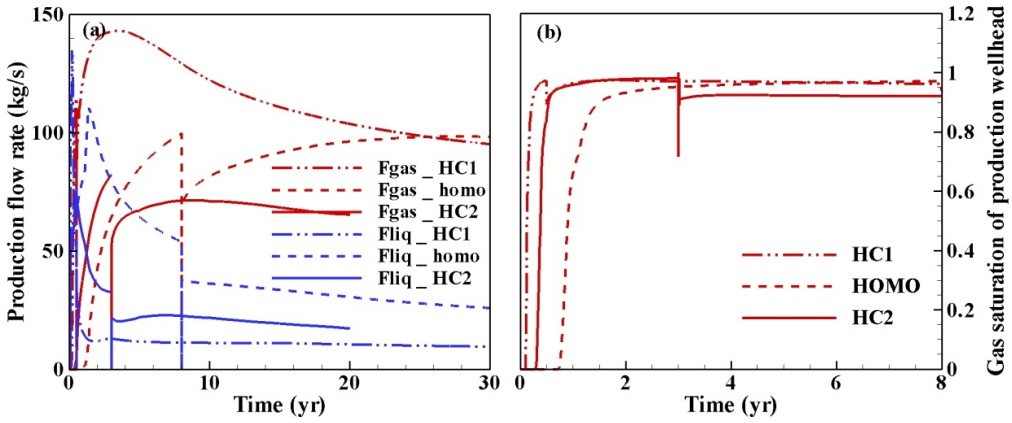

Fig. 12 Evolution of production flow rate (a) and gas saturation of production fluid (b)

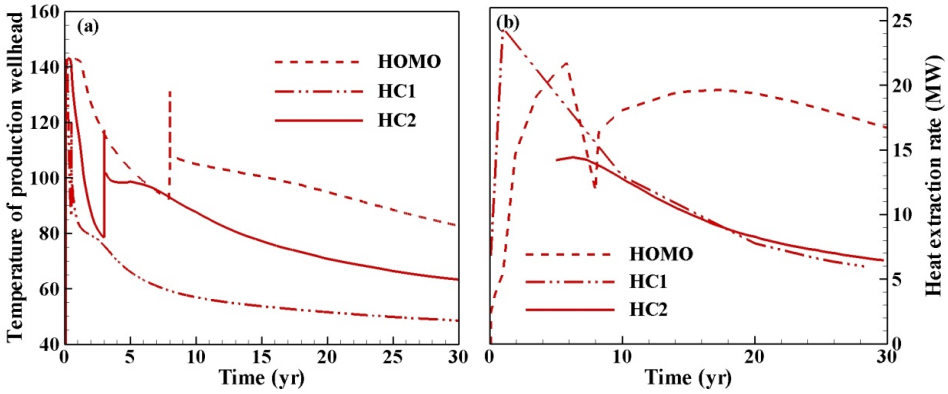

Fig. 13 Evolution of production fluid temperature and heat extraction rate

Production fluid temperature and heat extraction rate for heterogeneity cases are much lower than those of homogeneity case (Fig. 13a and b). Because of the preferential flow, the fluid cannot be heated sufficiently. In addition, the heat-exchange volume is smaller than the homogeneity one. In the late stage, there is a large decline of production fluid temperature, especially for HC1, which corresponds to the shortest circulation time and least heat-exchange volume.

3 Conclusions

The wellbore-reservoir coupled numerical simulations for a CO_2-based geothermal system were performed in this paper, based on the geological and thermo-physical condition of the Songliao Basin of China. From the numerical analysis the following conclusions can be drawn.

For "two-spot" well pattern, the main pressure loss is in the reservoir, not the frictional loss in wellbore. Because the boundary is not closed, it leads to pressure dispersion. Frictional pressure loss in production is higher than that in injection well due to lower density and higher velocity. Under the condition of same injection pressure, increases of the production pressure help to increase the production fluid temperature and lessen the frictional loss.

For the heterogeneity cases, due to the strong mobility of CO_2, as long as there exists highly permeable zone between the two wells, even the flow path is much longer, it is more likely to flow through the highly permeable zone to reach the production well. The preferential flow can largely shorten the circulation time and reduce the heat-exchange area, probably leading to early thermal breakthrough, which makes the production fluid temperature decrease rapidly. Therefore, in future field project, we should try to avoid strongly heterogeneous geothermal reservoir.

Acknowledgements

This work was supported by the National Natural Science Foundation of China (Grant No. 41272254 and No. 41572215).

References

Archie G E. 1950. Introduction to petrophysics of reservoir rocks. AAPG Bulletin, 34(5): 943-961.

Archie G E. 1952. Classification of carbonate reservoir rocks and petrophysical considerations. AAPG Bulletin, 36(2): 278- 298.

Atrens A D, Gurgenci H, Rudolph V. 2010. Electricity generation using a carbon-dioxide thermosiphon. Geothermics, 39(2): 161-169.

Baecher G B, Christian J T. 2005. Reliability and statistics in geotechnical engineering. Chichester: John Wiley & Sons.

Bear J. 1972. Dynamics of fluids in porous media. New York: Dover Publications.

Brown D W. 2000. A hot dry rock geothermal energy concept utilizing supercritical CO_2 instead of water. In: Proceedings of the twenty-fifth workshop on geothermal reservoir engineering. Palo Alto: Stanford University, 233-238.

Carman P C. 1956. Flow of gases through porous media. Cambridge: Academic Press.

Curran P J. 1988. The semivariogram in remote sensing: an introduction. Remote Sensing of Environment, 24(3): 493-507.

Davis S N. 1969. Porosity and permeability of natural materials. New York: Flow through Porous Media, 53-89.

Ehrenberg S N, Nadeau P H. 2005. Sandstone vs. carbonate petroleum reservoirs: A global perspective on porosity-depth and porosity-permeability relationships. AAPG Bulletin, 89(4): 435-445.

Haldar S, Babu G L S. 2008. Effect of soil spatial variability on the response of laterally loaded pile in undrained clay. Computers and Geotechnics, 35(4): 537-547.

Katz A J, Thompson A H. 1986. Quantitative prediction of permeability in porous rock. Physical Review B, 34(11): 8179.

Nelson P H. 1994. Permeability-porosity relationships in sedimentary rocks. The Log Analyst, 35(3): 38-62.

Pan L, Freifeld B, *et al*. 2015. Fully coupled wellbore-reservoir modeling of geo-thermal heat extraction using CO_2 as the working fluid. Geothermics, 53: 100-113.

Pan L, Oldenburg C M. 2014. T2Well-an integrated wellbore-reservoir simulator. Computers &

Geosciences, 65: 46-55.

Pan L, Oldenburg C M, *et al*. 2011a. Transient CO_2 leakage and injection in wellbore-reservoir systems for geologic carbon sequestration. Greenhouse Gases: Science and Technology, 1(4): 335-350.

Pan L, Oldenburg, C M, *et al*. 2011b. T2Well/ECO2N version 1.0: Multiphase and non-isothermal model for coupled wellbore-reservoir flow of carbon dioxide and variable salinity water, LBNL-4291E. Berkeley: Lawrence Berkeley National Laboratory.

Pruess K. 2006. Enhanced geothermal systems (EGS) using CO_2 as working fluid–A novel approach for generating renewable energy with simultaneous sequestration of carbon. Geothermics, 35(4): 351-367.

Pruess K. 2008. On production behavior of enhanced geothermal systems with CO_2 as working fluid. Energy Conversion and Management, 49(6): 1446-1454.

Pruess K, Oldenburg C, Moridis G. 1999. TOUGH2 user's guide, version 2.0 report LBNL-43134. Berkeley: Lawrence Berkeley National Laboratory, Earth Sciences Division.

Ramey Jr H J. 1962. Wellbore heat transmission. Journal of Petroleum Technology, 14(04): 427-435.

Randolph J B, Saar M O. 2011. Coupling carbon dioxide sequestration with geothermal energy capture in naturally permeable, porous geologic formations: Implications for CO_2 sequestration. Energy Procedia, (4): 2206-2213.

Srivastava A, Babu G L S, Haldar S. 2010. Influence of spatial variability of permeability property on steady state seepage flow and slope stability analysis. Engineering Geology, 110(3): 93-101.

Tester J W, Anderson B, *et al.* 2006. The future of geothermal energy: Impact of enhanced geothermal systems (EGS) on the United States in the 21st century. Massachusetts: Massachusetts Institute of Technology, 209.

TIAN H, PAN F, *et al*. 2014. Impacts of hydrological heterogeneities on caprock mineral alteration and containment of CO_2 in geological storage sites. International Journal of Greenhouse Gas Control, (24): 30-42.

Timur, A. 1968. An investigation of permeability, porosity, and residual water saturation relationships, SPWLA 9th annual logging symposium. New Orleans: Society of Petrophysicists and Well-Log Analysts.

XU T, FENG G, *et al.* 2015. Wellbore–reservoir coupled simulation to study thermal and fluid processes in a CO_2-based geothermal system: Identifying favorable and unfavorable conditions in comparison with water. Environmental Earth Sciences, 73(11): 6797-6813.

Zimmerman D L, Zimmerman M B. 1991. A comparison of spatial semivariogram estimators and corresponding ordinary kriging predictors. Technometrics, 33(1): 77-91.